Journal of Applied Physics ARTICLE scitation.org/journal/jap

Degradation of InGaN-based LEDs: Demonstration of a recombination-dependent defect-generation process

Cite as: J. Appl. Phys. **127**, 185701 (2020); doi: 10.1063/1.5135633
Submitted: 11 November 2019 · Accepted: 23 April 2020 ·
Published Online: 8 May 2020

N. Renso, C. De Santi, A. Caria, F. Dalla Torre, L. Zecchin, G. Meneghesso, E. Zanoni, and M. Meneghini[a)]

AFFILIATIONS

Department of Information Engineering, University of Padova, via Gradenigo 6/B, 35131 Padova, Italy

[a)]**Author to whom correspondence should be addressed:** matteo.meneghini@dei.unipd.it

ABSTRACT

This paper provides insights into the degradation of InGaN-based LEDs by presenting a comprehensive analysis carried out on devices having two quantum wells (QWs) with different emission wavelengths (495 nm and 405 nm). Two different configurations are considered: one with the 495 nm QW closer to the p-side and one with the 495 nm QW closer to the n-side. The original results collected within this work indicate that (i) during stress, the devices show an increase in defect-related leakage both in reverse and low-forward voltage ranges: current increases with the square-root of stress time, indicating the presence of a diffusion process; (ii) stress induces a decrease in the luminescence signal emitted by both quantum wells: the drop in luminescence is stronger when measurements are carried out at low current levels, indicating that degradation is due to the generation of Shockley–Read–Hall recombination centers; (iii) remarkably, the degradation rate is linearly dependent on the luminescence signal emitted before stress by the well, indicating that carrier density impacts on degradation; and (iv) the optical degradation rate has a linear dependence on the stress current density. The results strongly suggest the existence of a recombination-driven degradation process: the possible role of Shockley–Read–Hall and Auger recombination is discussed. The properties of the defects involved in the degradation process are described through steady-state photocapacitance measurements.

I. INTRODUCTION

InGaN-based light-emitting diodes (LEDs) have emerged as excellent devices for application in lighting and, more recently, for displays and micro-displays. Contrary to lighting applications, where high luminous fluxes are required, for the display field, it is required that the LEDs can be dimmed to very low light intensities, while maintaining efficient and stable output. At low current densities, e.g., below 1–10 A/cm^2, the optical characteristics of the devices are dominated by the Shockley–Read–Hall (SRH) recombination, whose rate is proportional to the density of defects (N_T), the capture cross section (σ_n), and the thermal velocity of the carriers (v_{th}). Recent studies[1–3] pointed out that during constant current operation, the optical power (OP) emitted by the LEDs can show a measurable decrease. In several cases, degradation impacts on the low-current efficiency of the LEDs, which is particularly critical for display applications. Degradation was ascribed to the generation of defects within the active region of the devices;[1–3] early papers[4–6] on laser diodes confirmed this hypothesis.

However, to date, several questions are still unanswered: what is the root mechanism for degradation? How does the degradation rate depend on carrier density in each well? Is the density of defects near the quantum well (QW) region effectively increasing during stress?

II. AIM AND EXPERIMENTAL DETAILS

The goal of this paper is to address these questions by demonstrating that (i) degradation of the electrical characteristics of InGaN-based LEDs follows the square-root of stress time, supporting the hypothesis on defect diffusion; (ii) the degradation rate is dependent on the initial luminescence of the quantum well; QWs with higher initial luminescence show the strongest OP drop, suggesting the existence of a recombination-driven degradation mechanism; (iii) the degradation rate has a linear dependence on stress current; and (iv) optical degradation is correlated to an increase in defect density, as shown by steady-state photocapacitance (SSPC) measurements.

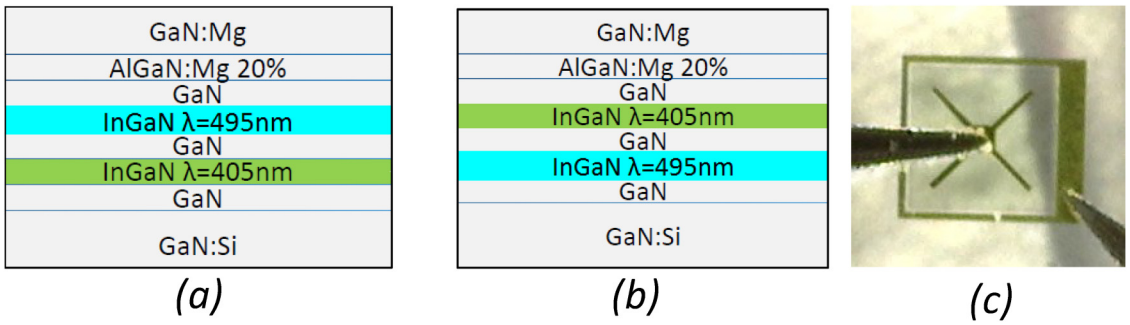

FIG. 1. (a) and (b) Structure of the two analyzed color-coded samples. Both devices have two quantum wells; the position of the 495 nm quantum well is changed (close to the p-side or close to the n-side). (c) Picture of one of the analyzed devices. Effective area is 500 × 500 μm^2.

To this aim, we designed an experiment based on color-coded quantum wells. The benefit of having a color-coded structure as a "test" device is that, in the case of multiple QWs, one can identify from which QW the light is generated, by detecting its wavelength. Two different test structures were fabricated on 2 in. sapphire substrates by metalorganic chemical vapor deposition (MOCVD, see Fig. 1) on 3 μm GaN templates; both structures have two quantum wells, emitting at different wavelengths. The QW emitting at 495 nm is referred to as the reference quantum well, since this is the one showing the strongest emission. The QW emitting at 405 nm is referred to as the secondary quantum well. In the structure in Fig. 1(a), the reference QW is located closer to the p-side, while in the structure in Fig. 1(b), it is located closer to the n-side.

The devices were submitted to constant current stress at 200 mA (80 A/cm^2), at room temperature [room temperature (RT), 25 °C]. Temperature was controlled with a Peltier-based system. During stress, the electrical characteristics of the devices were monitored by means of two-wire high-sensitivity current–voltage (I–V) measurements, while the optical and spectral characteristics were analyzed by means of a compact array spectrometer (CAS) with a cooled detector.

III. RESULTS AND DISCUSSION

Figure 2(a) reports the current–voltage characteristics of one of the stressed devices [with the structure shown in Fig. 1(a)], collected before and during stress at 200 mA. As can be noticed, stress induced a significant increase in both reverse current and subturn-on forward leakage (in the voltage range between 1 and 2.5 V). In both voltage ranges, conduction is mainly dominated by defect-assisted mechanisms. The second structure showed an analog behavior, suggesting that the different QWs' structure does not impact on the electrical properties of the tested devices.

In the reverse-bias regime, hopping (either variable-range hopping, VRH, or nearest-neighbor hopping, NNH) typically dominates;[7–10] the contribution of thermally assisted multistep tunneling has also been proposed to contribute .[8] As a consequence, reverse conduction is strongly dependent on the density of defects within the depleted region or, equivalently, on the distance between neighboring traps. An analytical model was recently proposed in Ref. 9, according to which reverse leakage due to VRH and NNH can be expressed as

$$J(F, T) \propto D_x \exp\left(-\frac{4\sqrt{2m^*}\varepsilon^{\frac{3}{2}}}{3qF\hbar}\right) \exp\left[-\left(\frac{T_0}{T}\right)^{\nu}\right],$$

where D_x is the volume density of unoccupied states at point x, F is the maximum electric field in the depletion region, and T_0 is a characteristic temperature.

In the low-forward bias regime (here between 1 and 2.5 V), conduction is mostly dominated by trap-assisted tunneling, as demonstrated by recent papers (see, for instance, Ref. 11). Also in this regime, the defect-mediated current is proportional to the density of defects (see, for instance, Ref. 12) where the following

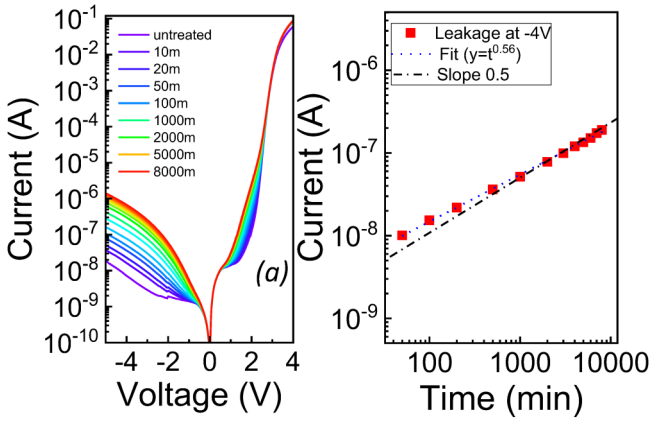

FIG. 2. (a) Current–voltage measurements collected on one of the analyzed samples with the structure reported in Fig. 1 (a) during stress at 200 mA. Relevant changes are detected both in the reverse and low-forward voltage leakage. (b) Change in the reverse leakage (measured at −4 V). Leakage current increases with the square-root of stress time.

formula has been proposed:

$$J \propto \frac{qN_T}{E} \int f(\phi) d\phi,$$

where $f(\phi)$ is a function describing the shape and properties of the tunneling barrier (details can be found in Ref. 12).

As shown in Fig. 2(b), during stress the reverse leakage of the devices showed a monotonic increase, indicating a gradual increase in the density of defects within the active region. Remarkably, reverse leakage increased with the square-root of stress time. The slight deviation from the ideal $t^{0.5}$ curve could be possibly ascribed to the presence of a competing degradation process in the initial phase of stress, which is not relevant for long stress times. Here, the hypothesis is that the leakage increase is due to the increase in the defect density in the depleted region due to a diffusion process, in agreement with previous papers on laser diodes.[4–6] Possible diffusing defects may be hydrogen,[2,13,14] hydrogen/oxygen vacancy complexes,[15,16] magnesium,[4,17,18] or intrinsic defects as vacancy complexes.[15,19,20]

The degradation of the optical characteristics of the devices was investigated by electroluminescence measurements [Fig. 3(a)]: optical power degradation was detected only in the low (measurement) current regime (below 1 mA), i.e., in the current range where recombination efficiency is limited by SRH losses and the slope of the log–log L-I plot is nearly equal to 2.[21]

We analyzed the spectral and electroluminescence (EL) characteristics of the two sets of LEDs, those with the 495 nm QW closer to the p-side and those with the 495 nm QW closer to the n-side. The results are shown in Figs. 3(b), 3(c), and 4. It is worth noticing that for the structure with the 495 nm QW close to the p-side, no emission from the 405 nm QW is detected at RT, due to the relative position of the Fermi level in the two quantum wells that favor emission from the 495 nm QW only. Hence, the carrier density within the two QWs is not equal.

Both QWs showed a decrease in luminescence intensity during stress time. As shown in Fig. 3(a), the effect of degradation was stronger at low measuring current levels. This confirms that the drop in optical power is due to an increase in the SRH recombination rate that has a stronger impact at low current densities. An analysis of the degradation data indicates that OP degradation does not follow a square-root dependence on time. Thus, we conclude that the diffusion process responsible for the changes in the electrical characteristics of the samples is not the dominant cause for optical degradation, in the devices under investigation; the diffusing defects do not act as the main recombination centers but can enhance the parasitic leakage conduction. This difference may be related to their energy position inside the energy gap: to be effective recombination centers, they need to be close to midgap, a condition not mandatory for trap-assisted current conduction.

To study the origin of optical degradation, we analyzed the correlation between the spectral data and the degradation rate (Figs. 3 and 4) for 405 nm and 495 nm QWs in the two positions. In Fig. 4, one can easily notice that the degradation is stronger when the reference QW is close to the p-side. Interestingly, the results indicated a correlation between the initial luminescence of a given well and its degradation rate: this is summarized by Fig. 4(c) that reports the OP drop (measured at 100 μA, after 1000 min of stress, at the peak wavelength) as a function of the initial QW

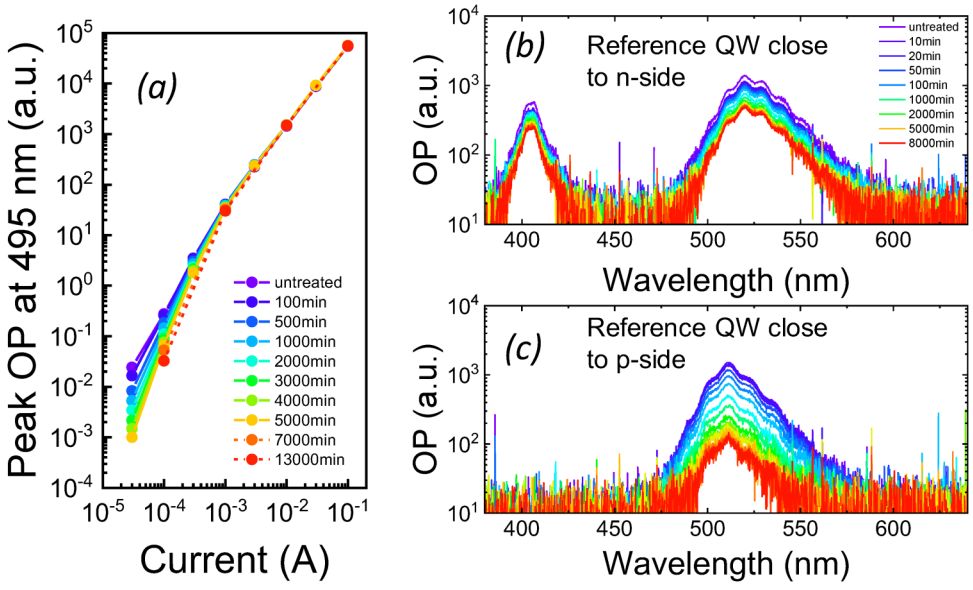

FIG. 3. (a) Optical power vs current characteristics measured during a stress experiment on the 495 nm quantum well (device with 495 nm QW closer to the p-side). (b) EL spectra measured at 100 μA during stress on the sample with the 495 nm QW (b) closer to the n-side and (c) closer to the p-side.

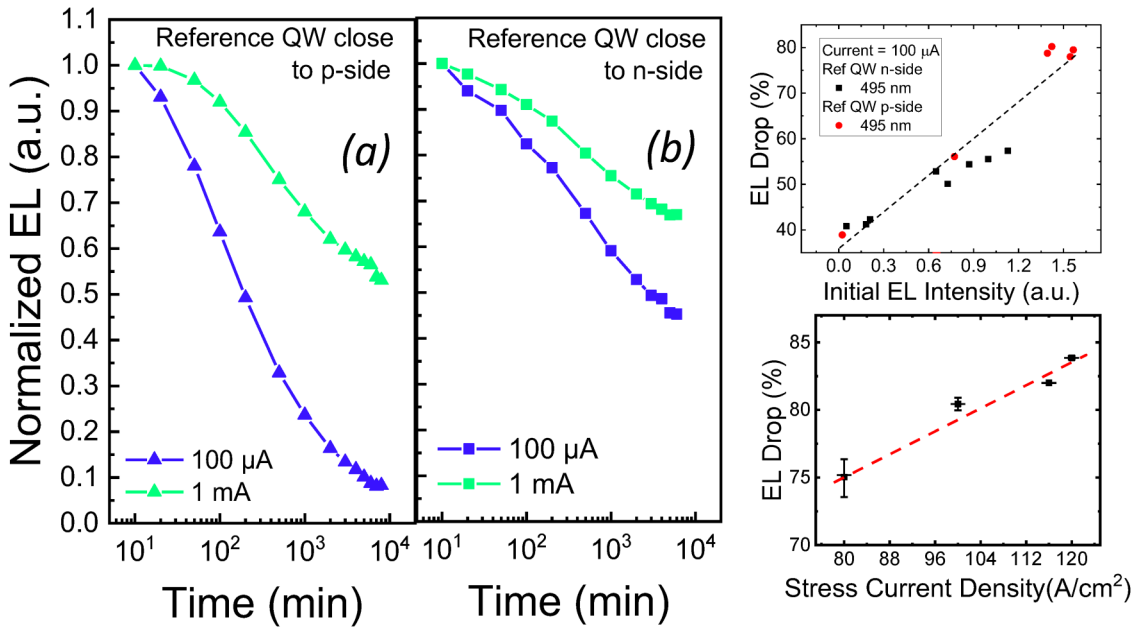

FIG. 4. Normalized EL signal collected from the 495 nm QW during stress time for the structures with 495 nm QW (a) close to the p-side and (b) close to the n-side. Dependence of optical degradation (measured at 100 μA, after 1000 min of stress) (c) on the initial EL intensity and (d) on the stress current density (lines are guides to the eye). In (c) and (d), samples of both the variants were used to build up the graph: each point in (d) represents the average EL drop for a specific stress current density.

luminescence. The EL differences among different samples on the same wafer are related to device-to-device fluctuations, and they are not related to intentional modifications of the samples structure. Note that all the EL data reported in Fig. 4 were obtained at 100 μA, a current where EL intensity is strongly influenced by defect density. As can be noticed, QWs with higher initial luminescence show the strongest degradation rate. Figure 4(c) demonstrates that the degradation rate has a linear dependence on the initial EL intensity, which, in turn, depends on the carrier density. Based on these results, we conclude that carrier density impacts on the degradation rate. A possible interpretation of the data is discussed in the following. During stress at high current densities, two dominant non-radiative processes may occur in the well: SRH and Auger recombination. SRH recombination depends linearly on carrier density, while Auger recombination scales with n^3. Each SRH and Auger recombination event releases an energy close to the bandgap, which may be sufficient to break defect–impurity bonds in GaN (see, for instance, Refs. 15 and 22), thus promoting the generation of defects in the quantum wells.

To understand if degradation is promoted by SRH or Auger recombination, we consider that the rate of injection is proportional to I/(qdLW), where I is current, q is the electron charge, and d, L, and W are the depth, length, and width of the active region. In a simple ABC model approach, the rate equation is expressed by

$$I/(qdLW) = An + Bn^2 + Cn^3,$$

where A, B, and C represent the SRH, bimolecular, and Auger recombination rates, respectively. By considering typical values for the A, B, and C coefficients ($A = 10^6\ s^{-1}$, $B = 10^{-12}\ cm^3/s$, and $C = 10^{-31}\ cm^3/s$, see, for instance, Ref. 23), at the stress current level of 200 mA, Auger recombination accounts for 66% of total recombination rate, while SRH accounts for 1.4% [Fig. 5(a)]. Based on this consideration, we suggest that the energy released by Auger recombination may favor the defect generation process responsible for the OP degradation.[24]

By carrying out stress tests at different current levels [Fig. 4(d)], we further confirmed the role of carrier density in the degradation process: degradation rate (OP drop after 1000min of stress) was found to have a linear dependence on stress current level [Fig. 4(d)]. According to the rate equation reported above, near the stress current level (200 mA), Auger recombination rate has a linear dependence on current [Fig. 5(b)], because of very high current, $I/(qdLW) \sim Cn^3$. On the other hand, bimolecular and SRH recombination rates have a sub-linear dependence on current [Figs. 5(a) and 5(b)]. The results in Fig. 4(d), therefore, support the hypothesis of a role of Auger recombination in favoring the degradation process. Device self-heating related to the high stress current density may also play a role, enhancing the degradation kinetics.[25,26]

To be more specific on the properties of the defects involved in the degradation process, we carried out SSPC measurements with increasing stress times. SSPC measurements [Fig. 6(a)] monitor the device capacitance variation induced by the exposure to a monochromatic light. If the energy of the monochromatic

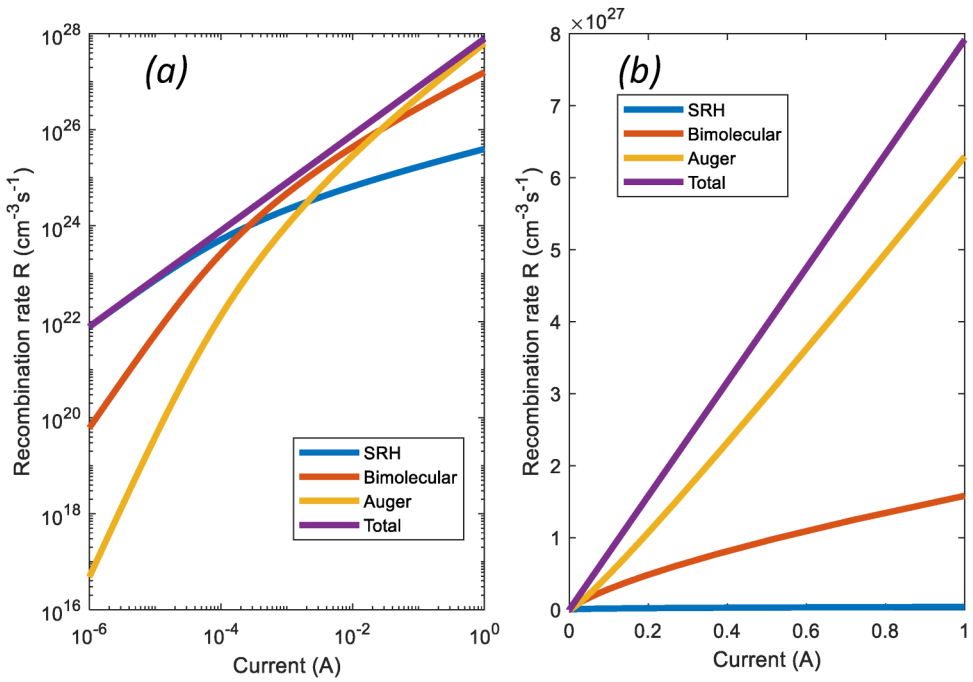

FIG. 5. SRH, bimolecular, Auger, and total recombination rates as a function of driving current for a LED with recombination coefficients equal to A = 10^{6} s^{-1}, B = 10^{-12} cm^3/s, C = 10^{-31} cm^3/s. A simple ABC model is used for the calculations.

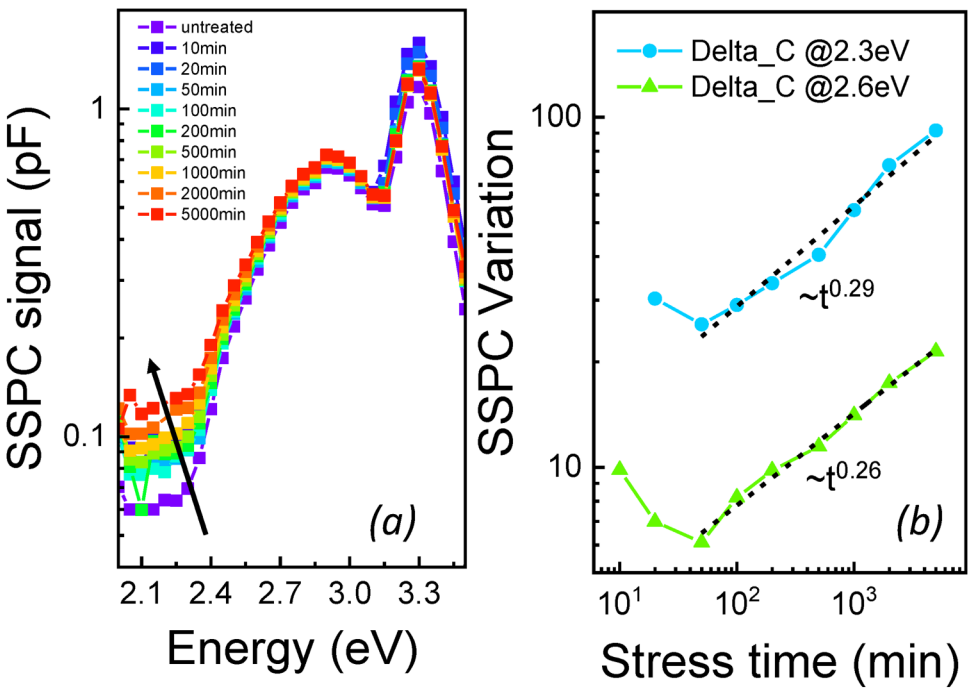

FIG. 6. (a) Variation of SSPC signal measured during stress on one of the analyzed samples. (b) Time-variation of the SSPC signal during stress time, monitored at 2.3 eV and 2.6 eV.

photons is large enough, trapped carriers will be released, inducing a variation in the device capacitance (typically an increase, if majority carriers are involved) and a consequent step in the SSPC curves. During the SSPC measurements, the sample was biased at 0 V, in order to investigate the density of defects in and near the active region (for further details, see Ref. 27). The results are reported in Figs. 6(a) and 6(b): one needs to consider the spectral range below 2.6–2.7 eV, since above this, energy generation in the QWs becomes relevant, thus covering defect-generated signals. As can be noticed, stress induced an increase in the density of deep levels within the active region of the devices; such an increase is particularly noticeable for energies lower than 2.3 eV (corresponding to defects located between midgap and E_C −2.3 eV). Albeit the measurement sensitivity was not enough for clearly estimating the energy position of such levels, the results support the hypothesis that stress induced an increase in the density of deep traps. We suggest that such defects are located near midgap, since they act as efficient SRH centers, and they impact on the sub-threshold forward leakage (as predicted theoretically in Refs. 28 and 29). The possible origin of non-radiative defects may be nitrogen-related defects or vacancies,[30] complexes of gallium vacancies,[15] or divacancy ($V_{Ga}V_N$) complexes.[20]

IV. CONCLUSIONS

In summary, we investigated the processes responsible for the degradation of InGaN LEDs by using color-coded test structures. The results indicate the existence of a defect diffusion process that leads to the increase in the reverse leakage of the devices. Remarkably, carrier density (estimated by the initial QW luminescence) is found to have a strong impact on the degradation rate, demonstrating the existence of a recombination-driven degradation process. Results are interpreted by considering that stress induces an increase in the density of SRH centers in the quantum wells; the generation of defects is proved through SSPC measurements. Degradation is suggested to be initiated by Auger recombination.

ACKNOWLEDGMENTS

Part of this work was supported by MIUR (Italian Minister for Education) under the initiative "Departments of Excellence" (Law 232/2016).

REFERENCES

[1]Z. Ma, H. Cao, S. Lin, X. Li, and L. Zhao, "Degradation and failure mechanism of AlGaN-based UVC-LEDs," Solid State Electron. **156**(January), 92–96 (2019).
[2]J. Glaab, J. Ruschel, T. Kolbe, A. Knauer, J. Rass, H. K. Cho, N. Lobo Ploch, S. Kreutzmann, S. Einfeldt, M. Weyers, and M. Kneissl, "Degradation of (In) AlGaN-based UVB LEDs and migration of hydrogen," IEEE Photonics Technol. Lett. **31**(7), 529–532 (2019).
[3]J. Ruschel, J. Glaab, M. Brendel, J. Rass, C. Stölmacker, N. Lobo-Ploch, T. Kolbe, T. Wernicke, F. Mehnke, J. Enslin, S. Einfeldt, M. Weyers, and M. Kneissl, "Localization of current-induced degradation effects in (InAlGa) N-based UV-B LEDs," J. Appl. Phys. **124**(8), 084504 (2018).
[4]K. Orita, M. Meneghini, H. Ohno, N. Trivellin, N. Ikedo, S. Takigawa, M. Yuri, T. Tanaka, E. Zanoni, and G. Meneghesso, "Analysis of diffusion-related gradual degradation of InGaN-based laser diodes," IEEE J. Quantum Electron. **48**(9), 1169–1176 (2012).
[5]S. Tomiya, T. Hino, S. Goto, M. Takeya, and M. Ikeda, "Dislocation related issues in the degradation of GaN-based laser diodes," IEEE J. Sel. Top. Quantum Electron. **10**(6), 1277–1286 (2004).
[6]P. Perlin, L. Marona, M. Leszczynski, T. Suski, P. Wisniewski, R. Czernecki, and I. Grzegory, "Degradation mechanisms of InGaN laser diodes," Proc. IEEE **98**(7), 1214–1219 (2010).
[7]S. Zhou, Y. Wu, Y. Zhang, C. Zheng, S. Liu, and J. Lv, "Reverse leakage current characteristics of InGaN/GaN multiple quantum well ultraviolet/blue/green light-emitting diodes," Jpn. J. Appl. Phys. **57**(5), 051003 (2018).
[8]Q. Shan, D. S. Meyaard, Q. Dai, J. Cho, E. Fred Schubert, J. Kon Son, and C. Sone, "Transport-mechanism analysis of the reverse leakage current in GaInN light-emitting diodes," Appl. Phys. Lett. **99**(25), 2009–2012 (2011).
[9]L. Zhao, L. Chen, G. Yu, D. Yan, G. Yang, X. Gu, B. Liu, and H. Lu, "Tunneling-hopping transport model for reverse leakage current in InGaN/GaN blue light-emitting diodes," IEEE Photonics Technol. Lett. **29**(17), 1447–1450 (2017).
[10]M. Lee, H. U. Lee, K. M. Song, and J. Kim, "Significant improvement of reverse leakage current characteristics of Si-based homoepitaxial InGaN/GaN blue light emitting diodes," Sci. Rep. **9**(1), 1–6 (2019).
[11]W. A. Quitsch, D. Sager, M. Loewenich, T. Meyer, B. Hahn, and G. Bacher, "Low injection losses in InGaN/GaN LEDs: The correlation of photoluminescence, electroluminescence, and photocurrent measurements," J. Appl. Phys. **123**(21), 214502 (2018).
[12]D. M. Sathaiya and S. Karmalkar, "Thermionic trap-assisted tunneling model and its application to leakage current in nitrided oxides and AlGaN/GaN high electron mobility transistors," J. Appl. Phys. **99**(9), 093701 (2006).
[13]C. De Santi, M. Meneghini, G. Meneghesso, and E. Zanoni, "Degradation of InGaN laser diodes caused by temperature- and current-driven diffusion processes," Microelectron. Reliab. **64**, 623–626 (2016).
[14]C. H. Seager, S. M. Myers, A. F. Wright, D. D. Koleske, and A. A. Allerman, "Drift, diffusion, and trapping of hydrogen in p-type GaN," J. Appl. Phys. **92**(12), 7246–7252 (2002).
[15]C. E. Dreyer, A. Alkauskas, J. L. Lyons, J. S. Speck, and C. G. Van de Walle, "Gallium vacancy complexes as a cause of Shockley-Read-Hall recombination in III-nitride light emitters," Appl. Phys. Lett. **108**(14), 141101 (2016).
[16]J. L. Lyons, A. Alkauskas, A. Janotti, and C. G. Van de Walle, "First-principles theory of acceptors in nitride semiconductors," Phys. Status Solidi B **252**(5), 900–908 (2015).
[17]I. S. Romanov, I. A. Prudaev, A. A. Marmalyuk, V. A. Kureshov, D. R. Sabitov, and A. V. Mazalov, "Effect of magnesium diffusion into the active region of LED structures with InGaN/GaN quantum wells on internal quantum efficiency," Russ. Phys. J. **57**(4), 533–535 (2014).
[18]L. Kirste, K. Köhler, M. Maier, M. Kunzer, M. Maier, and J. Wagner, "SIMS depth profiling of Mg back-diffusion in (AlGaIn)N light-emitting diodes," J. Mater. Sci. Mater. Electron. **19**, 176–181 (2008).
[19]S. F. Chichibu, K. Shima, K. Kojima, S. Takashima, K. Ueno, M. Edo, H. Iguchi, T. Narita, K. Kataoka, S. Ishibashi, and A. Uedono, "Room temperature photoluminescence lifetime for the near-band-edge emission of epitaxial and ion-implanted GaN on GaN structures," Jpn. J. Appl. Phys. **58**, SC0802 (2019).
[20]S. F. Chichibu, A. Uedono, K. Kojima, H. Ikeda, K. Fujito, S. Takashima, M. Edo, K. Ueno, and S. Ishibashi, "The origins and properties of intrinsic nonradiative recombination centers in wide bandgap GaN and AlGaN," J. Appl. Phys. **123**(16), 161413 (2018).
[21]O. Pursiainen, N. Linder, A. Jaeger, R. Oberschmid, and K. Streubel, "Identification of aging mechanisms in the optical and electrical characteristics of light-emitting diodes," Appl. Phys. Lett. **79**(18), 2895–2897 (2001).
[22]I. S. Romanov, I. A. Prudaev, and V. N. Brudnyi, "Diffusion of magnesium in LED structures with InGaN/GaN quantum wells at true growth temperatures 860–980 °C of p-GaN," Russ. Phys. J. **61**(1), 187–190 (2018).
[23]A. David, N. G. Young, C. A. Hurni, and M. D. Craven, "Quantum efficiency of III-nitride emitters: Evidence for defect-assisted nonradiative recombination and its effect on the green gap," Phys. Rev. Appl. **11**(3), 031001 (2019).

[24]J. Iveland, L. Martinelli, J. Peretti, J. S. Speck, and C. Weisbuch, "Direct measurement of auger electrons emitted from a semiconductor light-emitting diode under electrical injection: Identification of the dominant mechanism for efficiency droop," Phys. Rev. Lett. **110**(17), 1–5 (2013).
[25]M. Dal Lago, M. Meneghini, N. Trivellin, G. Meneghesso, and E. Zanoni, "Degradation mechanisms of high-power white LEDs activated by current and temperature," Microelectron. Reliab. **51**(9–11), 1742–1746 (2011).
[26]E. Jung and H. Kim, "Rapid optical degradation of GaN-based light-emitting diodes by a current-crowding-induced self-accelerating thermal process," IEEE Trans. Electron Devices **61**(3), 825–830 (2014).
[27]A. Chantre, G. Vincent, and D. Bois, "Deep-level optical spectroscopy in GaAs," Phys. Rev. B **23**(10), 5335–5359 (1981).
[28]M. Mandurrino, G. Verzellesi, M. Goano, M. Vallone, F. Bertazzi, G. Ghione, M. Meneghini, G. Meneghesso, and E. Zanoni, "Physics-based modeling and experimental implications of trap-assisted tunneling in InGaN/GaN light-emitting diodes," Phys. Status Solidi A **212**(5), 947–953 (2015).
[29]M. Auf Der Maur, B. Galler, I. Pietzonka, M. Strassburg, H. Lugauer, and A. Di Carlo, "Trap-assisted tunneling in InGaN/GaN single-quantum-well light-emitting diodes," Appl. Phys. Lett. **105**(13), 133504 (2014).
[30]M. Meneghini, M. La Grassa, S. Vaccari, B. Galler, R. Zeisel, P. Drechsel, B. Hahn, G. Meneghesso, and E. Zanoni, "Characterization of the deep levels responsible for non-radiative recombination in InGaN/GaN light-emitting diodes," Appl. Phys. Lett. **104**(11), 113505 (2014).